Research Article

Rapid and precise distance measurement with hybrid comb lasers

Zhichuang Wang,[a,b,†] Jiawen Zhi,[c,†] Hanzhong Wu,[c,†,*] Brent E. Little,[a] Sai T. Chu,[d] Jie Zhang,[c] Zehuang Lu,[c] Chenggang Shao,[c,*] Weiqiang Wang,[a,b,*] and Wenfu Zhang[a,b,*]

[a]Chinese Academy of Sciences, Xi'an Institute of Optics and Precision Mechanics, State Key Laboratory of Transient Optics and Photonics, Xi'an, China
[b]University of Chinese Academy of Sciences, Beijing, China
[c]Huazhong University of Science and Technology, PGMF and School of Physics, MOE Key Laboratory of Fundamental Physical Quantities Measurements, Hubei Key Laboratory of Gravitation and Quantum Physics, Wuhan, China
[d]City University of Hong Kong, Department of Physics and Materials Science, Hong Kong, China

Abstract. Dual-comb ranging allows rapid and precise distance measurement and can be universally implemented on different comb platforms, e.g., fiber combs and microcombs. To date, dual-fiber-comb ranging has become a mature and powerful tool for metrology and industry, but the measurement speed is often at a kilohertz level due to the lower repetition rates. Recently, dual-microcomb ranging has given rise to a new opportunity for distance measurement, in consequence of its small footprint and high repetition rates, but full-comb stabilization is challenging. Here, we report a dual-hybrid-comb distance meter capable of ultrarapid and submicrometer precision distance measurement, which can not only leverage the advantage of easy locking inherited from the fiber comb but also sustain ultrarapid measurement speed due to the microcomb. The experimental results show that the measurement precision can reach 3.572 μm at 4.136 μs and 432 nm at 827.2 μs averaging time. Benefiting from the large difference between the repetition rates of the hybrid combs, the measurement speed can be enhanced by 196 folds, in contrast to the dual-fiber-comb system with about a 250 MHz repetition rate. Our work can offer a solution for the fields of rapid dimensional measurement and spectroscopy.

Keywords: microcomb; absolute distance measurement; high-precision measurement; high-speed measurement.

1 Introduction

Precise length measurement has served a fundamental role in many fields, such as metrology, laser-based light detection and ranging (lidar), precision machining, deformation and posture measurement of large equipment, three-dimensional (3D) surface profilometry of micro-nano devices, and gravitational wave detection. Various optical methods have been proposed for distance measurement, and optical interferometry has been a powerful and well-established approach for high-precision measurement. Compared with incremental distance measurement, continuous detection is no longer necessary for absolute distance measurement. Therefore, absolute distance measurement has been extensively developed, based on the methods of time of flight and multiwavelength interferometry during the past several decades. For the scheme of time of flight, the precision could be limited by the time resolution of the measurement system. Taking into account the multiwavelength interferometry, the distances can be determined by exploiting a synthetic wavelength chain, while multiple laser sources are needed, leading to a complex and expensive system.[1]

Laser frequency combs, since their invention, have given rise to revolutionary progress in the field of metrology. Actually, the initial motivation of the frequency comb is to measure the optical frequency (hundreds of terahertz) with subhertz precision

*Address all correspondence to Hanzhong Wu, wuhanzhong@hust.edu.cn; Chenggang Shao, cgshao@hust.edu.cn; Weiqiang Wang, wangwqopt@163.com; Wenfu Zhang, wfuzhang@opt.ac.cn

[†]These authors contributed equally to this work.

($<10^{-14}$ in relative precision),[2] which is rather difficult when using the sophisticated frequency chain. When the two key parameters (repetition frequency f_{rep} and carrier-envelope-offset frequency f_{ceo}) are tightly locked to an external frequency reference, the frequency comb consequently becomes a stable ruler in both time and frequency domains. More importantly, the excellent frequency stability of the time base (microwave clocks or optical clocks) can be coherently transferred to the other frequencies with high fidelity, where frequency combs serve as a bidirectional bridge. Typically, this kind of comb laser can emit a femtosecond-pulse train with an ultrastable interval and therefore inherently provides a powerful tool for the time-of-flight measurement. In addition, frequency combs are composed of numerous coherent wavelengths and naturally support multiwavelength interferometry.[3] Inspired by these advantageous features, a variety of comb-based ranging methods have been proposed, such as pulse cross correlation,[4–6] dispersive interferometry,[7–10] intermode beat,[11,12] multiheterodyne interferometry,[13–15] dual-comb interferometry,[16–24] and pulse-to-pulse alignment.[25,26] At the moment, the distances can be already determined at long range with high precision and accuracy (approaching the quantum limit), large non-ambiguity range, and high speed.

Several mechanisms are capable of stimulating the frequency combs, such as passive mode locking,[27] electro-optics modulation,[28,29] quantum cascaded lasers,[30] and nonlinear evolution in microcavities.[31,32] By far, all these types of comb lasers can be self-referenced to the external frequency reference. Very recently, frequency combs based on microresonators (MRRs), also referred to as microcombs, have attracted extensive attention due to their small package, low power consumption, high repetition rate, large power of single tooth, broad bandwidth, and rich nonlinear phenomena.[33,34] Although the comb-based methods for distance measurement have been deliberated for a long time, microcombs could open a new window and offer new opportunities for the area of optical ranging. In 2021, Zheng et al. demonstrated the pulse cross correlation of microcombs for distance measurement.[35] With the high f_{rep} of microcombs, the mechanical stage with a small scanning range is sufficient to realize arbitrary distance measurement, also resulting in better mechanical stability in the meantime. In 2020, Wang et al. described dispersive interferometry in kilometer-level distance measurement with a fast spectrometer.[36] Because of the small pulse-to-pulse interval, the dead zones do not exist anymore. Subsequently, in 2021, Jang et al. demonstrated a hybrid method using soliton microcomb (SMC), which can support nanometric-precision distance metrology.[37] The non-ambiguity range can be extended by the amplified-spontaneous-emission dispersive interferometry, and the ultimate performance can be linked to the homodyne interferometry of one comb tooth. In 2018, Trocha et al. realized ultrafast distance measurement using dual-comb multiheterodyne interferometry.[38] A microwave comb can be coherently obtained whose phases can be used to measure the distances. As a consequence of the high f_{rep} of microcombs, a high update rate (close to 100 MHz) can be obtained, and a fast-moving target can be clearly captured after the data process based on the Fourier transform. In the same year, Suh et al. exploited dual-comb interferometry to measure distances with high precision, and Hilbert transform was used to pick up the peak position of the interferograms.[39] Particularly, the configuration of the common pump and common cavity maintains the high coherence between the two combs.

In 2020, Riemensberger et al. developed a frequency modulation continuous wave (FMCW) lidar using microcombs, and each comb tooth can work as one channel, giving rise to the 3D massive parallel ranging with one comb source.[40] Importantly, the sweep rate of the optical frequency can reach tens or even hundreds of megahertz, indicating the potential for future ultrafast microcomb lidar. However, a photodetector (PD) array is needed at the receiving side to acquire each individual channel. After that and in 2022, Lukashchuk et al. resolved this limitation by the dual-comb method, and 64 optical channels can be easily separated, although only one PD is designed.[41] In addition, microcombs can be also used as the calibrating source to monitor the optical frequency in traditional FMCW lidar[42] to further improve the measurement performance. As is well known, plenty of optical states (which are potentially useful to the distance measurement) can be experienced before reaching the SMC in the MRR. In 2023, the chaotic state was used to determine the distances based on the intensity cross correlation.[43,44] As a result of the excellent property of the intensity autocorrelation, the cross talk between the different channels can hardly be observed. The distance and the velocity can be simultaneously determined with millimeter-level precision. Although the precision could not achieve the micro- or nanometer region like the soliton state, chaos ranging has provided new ideas for microcomb applications.

Basically, microcombs can take charge of all the ranging methods demonstrated before. However, the full stabilization of microcombs is relatively challenging.[45,46] By far, the f_{rep} can be locked by feedback controlling the optical pump.[47–49] In another way, the passive injection locking via an electro-optic modulator (EOM) has been also demonstrated,[50,51] and the locking performance can track the frequency reference well. Nonetheless, the stabilization of the f_{ceo} of microcomb is not easy because the generation of the supercontinuum spectrum is difficult due to the low pulse peak power. Several groups have made great efforts to directly access the octave spectra by careful dispersion engineering,[52,53] giving rise to strong dispersive waves. Nevertheless, it is not easy to obtain the f_{ceo} signal with a high signal-to-noise ratio because of the relatively low power of the dispersive waves. Taking account of the microcomb ranging, optical distance measurement using a fully stabilized microcomb has not been demonstrated so far.

In this paper, we describe a ranging system involving two kinds of comb lasers, with submicrometer precision and hundreds of kilohertz update rate. With the help of one fully stabilized fiber comb, the pump laser can be locked to the hydrogen maser so as to lock the f_{ceo}. Since the f_{rep} (48.943783800 GHz) can be easily locked by injection locking, one fully stabilized microcomb source has been developed. We subsequently developed a ranging system with hybrid coherent comb lasers, microcomb, and fiber comb. Here, the fiber comb can not only serve as the bridge to the hydrogen maser but also operate as the local oscillator (LO) in dual-comb interferometry. The direct advantages of our system are the distance measurement can be traceable to the SI unit benefiting from the fully locked microcomb, and in addition, the high coherence between the microcomb and fiber comb can be maintained for a long term. As a result of the large difference between the repetition frequencies, the update rate of the hybrid-comb ranging system can be improved by hundreds of folds, in contrast to the dual-fiber-comb system with about a 250-MHz repetition rate. Our hybrid approach can not only leverage the advantage of being easy to lock (inherited

from the fiber comb) but also allow the ultrarapid measurement due to the microcomb.

2 Results

2.1 Fully Stabilized Single SMC Source

Figure 1 shows the experimental setup for the fully stabilized single SMC generation. A narrow-linewidth laser at 1560.49 nm is frequency-shifted by the acousto-optic modulator (AOM) and then is split into two beams. One beam passes through an intensity EOM working as the pump laser. The f_{rep} can be actively stabilized to the hydrogen maser using injection locking. The other beam is frequency-shifted by AOM, which acts as the auxiliary laser. The on-chip power of the two beams (pump laser and auxiliary laser) is boosted to ∼450 mW using two erbium-doped fiber amplifiers (EDFAs). The circulators inhibit the strong light from transmitting to the EDFAs. The single SMCs coupled out from the drop port are measured using an optical spectrum analyzer (OSA), a fast PD, and an electrical spectrum analyzer (ESA). The microwave sources used in the experiment are synchronized to the hydrogen maser. See the details in Sec. 4.1.

In our experiments, the single SMC is generated by the auxiliary-laser-based thermal balance method. The spectra of the microcomb has a sech^2 envelope with about a 100 nm optical spectral band, as shown in Fig. 2(a). To prevent the PD from saturating, the pump laser is filtered out using a fiber Bragg grating (FBG). The detected f_{rep} is amplified and mixed with the output of the signal generator (49 GHz) to obtain the beat signal, as shown in Fig. 2(b). When the repetition frequency is well locked, the signal-to-noise ratio can be improved to better than 70 dB, and the linewidth can be greatly narrowed, compared with the free-running case. The single-sideband (SSB) phase noise is then measured by a phase noise analyzer, as shown in Fig. 2(c). We find the SSB phase noise of the locked f_{rep} is −57 dBc/Hz at 1 Hz, which is reduced by about 97 dB compared to the free-running f_{rep}. When the offset frequency is larger than 30 kHz, the SSB phase noises are almost the same for both cases (the locked f_{rep} and the free-running f_{rep}). We then measure the locked f_{rep} for a long time to characterize the long-term stability with a frequency counter; the results are shown in Fig. 2(d). The standard deviation can reach 1.5 mHz in about 7000 s continuous measurement. The Allan deviation is 3.1×10^{-14} @ 1 s and 2.4×10^{-15} @ 100 s, as shown in Fig. 2(e), which is consistent with the stability of the signal generator referenced to the hydrogen maser. In contrast, the stability of the free-running f_{rep} is 2.1×10^{-9} @ 1 s and 4.8×10^{-9} @ 100 s. With the injection locking, the repetition frequency will follow the microwave frequency from the signal generator, which provides a new method for the fine adjustment of the repetition frequency. Figure 2(f) shows the results of the f_{rep} adjustment with
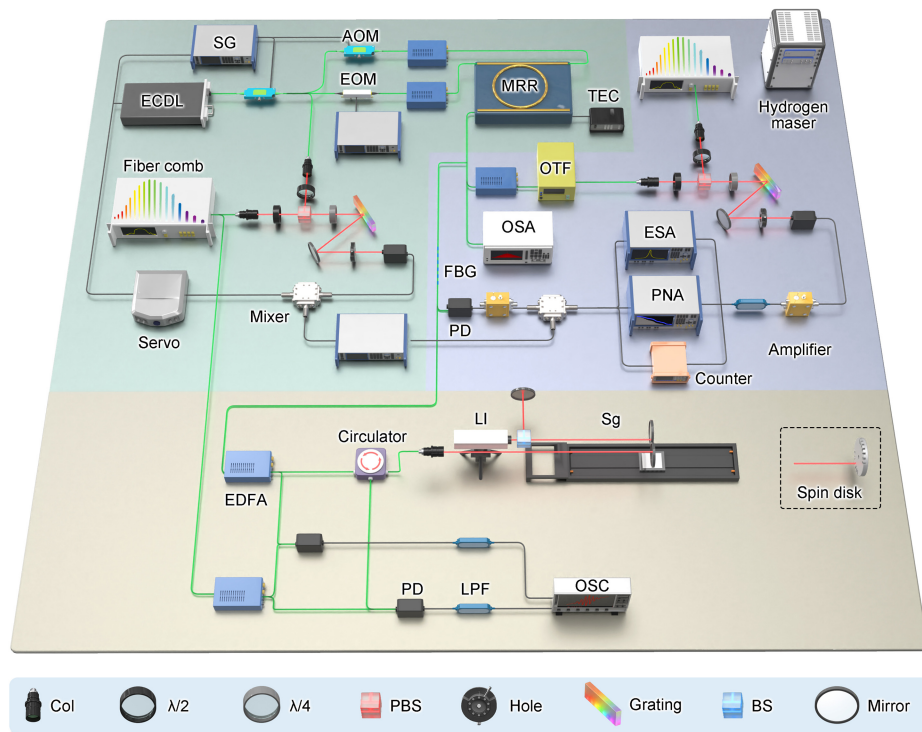

Fig. 1 Experimental setup. ECDL, external cavity diode laser; AOM, acousto-optic modulator; EOM, electro-optic modulator; EDFA, Er-doped fiber amplifier; MRR, microresonator; TEC, temperature controller; PD, photodetector; LPF, low-pass filter; PBS, polarization beam splitter; BS, beam splitter; FBG, fiber Bragg grating; OSA, optical spectrum analyzer; ESA, electrical spectrum analyzer; PNA, phase noise analyzer; OSC, oscilloscope; SG, signal generator; Servo, moku lab; OTF, optical bandpass filter; $\lambda/2$, half-wave plate; Col, collimator; $\lambda/4$, quarter-wave plate; LI, laser interferometer; Sg, sliding guide.
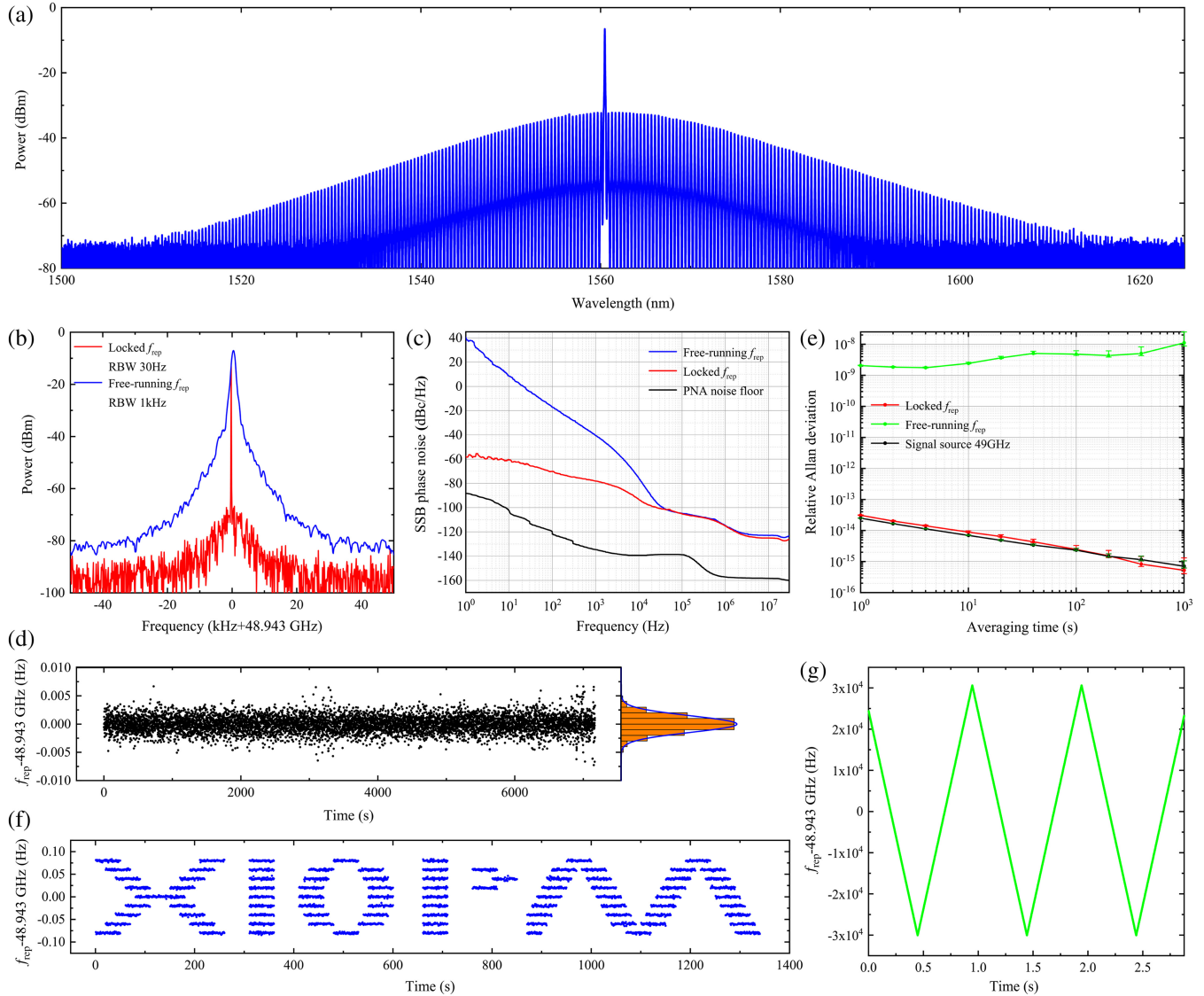
Fig. 2 Experimental results. (a) Optical spectrum of the single soliton. The spectrum of a sech² shape with about 100 nm optical band can be found. (b) Electrical spectrum of the free-running repetition frequency [blue, measured with 1 kHz resolution bandwidth (RBW)] and the locked repetition frequency (red, measured with 30 Hz RBW). (c) SSB phase noise of the free-running repetition frequency (blue) and the locked repetition frequency (red). The noise floor is shown as the black line. (d) The long-term measurement of the locked repetition frequency. The gate time of the frequency counter is 1 s. (e) Relative Allan deviation of the free-running repetition frequency (green), the locked repetition frequency (red), and the signal generator at 49 GHz (black). (f) The letters XIOPM obtained by programming the locked repetition frequency. (g) Linear modulation of the locked repetition frequency.

20 mHz step size, and the letters XIOPM (the abbreviation of Xi'an Institute of Optics and Precision Mechanics) can be depicted clearly. Figure 2(g) shows the linear modulation with 122 kHz/s speed and 61 kHz range. Robust and flexible control of the repetition rate is valuable for many applications.

Next, we try to lock the f_{ceo}. Since the pump laser is actually one of the comb teeth, we can lock the pump laser to the fully stabilized fiber comb. In this case, the single SMC can be fully stabilized. The in-loop beat frequency between the pump laser and the fiber comb is shown in Fig. 3(a), whose signal-to-noise

ratio can be well above 35 dB. Meanwhile, an additional fiber comb is used to beat with the SMC, to evaluate the noise and stability in the out loop. Figure 3(b) shows the out-loop beat frequency with about a 35-dB signal-to-noise ratio. We first measure the SSB phase noises of the pump laser, as shown in Fig. 3(c). After locking, the SSB phase noise of the pump laser is 30 dBc/Hz at 1 Hz offset frequency, which is actually reduced by 40 dB compared to the free-running situations. At the offset frequency from 10 Hz to 10 kHz, the SSB phase noises show similar values for both the free-running and the
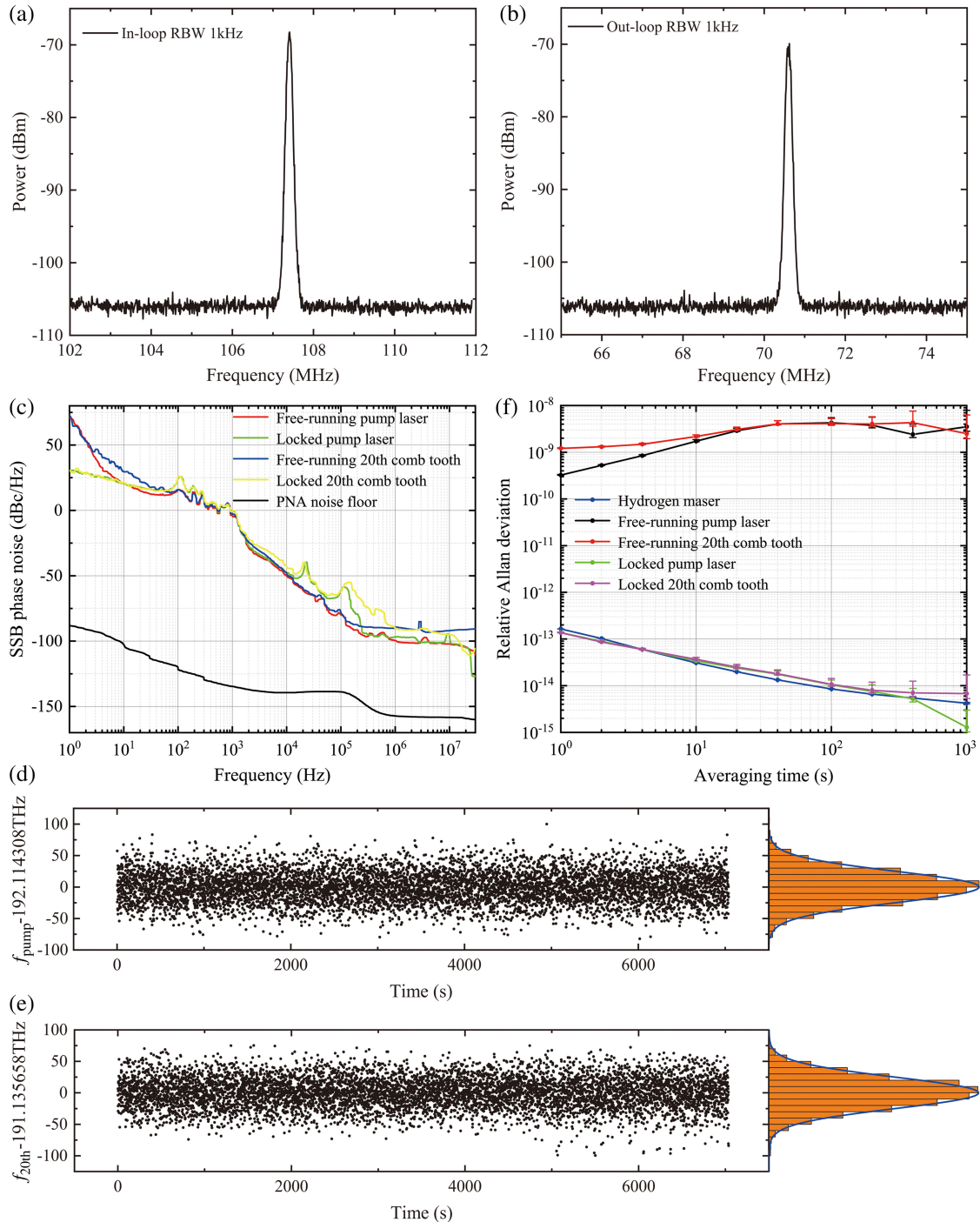
Fig. 3 Experimental results. (a) Electrical spectrum of the in-loop beat frequency between the pump laser and the fiber comb. The signal-to-noise ratio is better than 35 dB with 1 kHz RBW. (b) Electrical spectrum of the out-loop beat frequency between the pump laser and the additional fiber comb. The signal-to-noise ratio is 35 dB with 1 kHz RBW. (c) SSB phase noises of the free-running pump laser (red), the free-running 20th comb tooth (blue), the locked pump laser (green), and the locked 20th comb tooth (yellow). The noise floor is shown as the black line. (d) The long-term measurement of the locked pump laser with 1 s gate time. (e) The long-term measurement of the locked 20th comb tooth with 1 s gate time. (f) Relative Allan deviation of the free-running pump laser (black), the free-running 20th comb tooth (red), the locked pump laser (green), the locked 20th comb tooth (pink), and the hydrogen maser (blue).

locked cases. There are obvious phase noise spikes around 100 and 20 kHz due to the fast- and slow-loop servo systems bandwidth as well as the performance of electrical devices in the phase-locking loop.[54] The SSB phase noise of the 20th comb tooth (1568.48 nm) exhibits features similar to that of the pump laser, except that at the offset frequency larger than about 60 kHz, the noise is obviously higher than that of the pump laser. This is because the optical power of the 20th comb tooth is much lower, and two stages of optical power amplification are used to obtain the beat note with the fiber comb. In addition, the beat note is then electrically amplified so as to be identified by the phase noise analyzer. We consider that the optical and electrical power amplifications make great contributions to the phase noise at offset frequencies larger than 60 kHz.

In the stability evaluation, the long-term measurement result of the pump laser is shown in Fig. 3(d). We find the standard deviation of 24.83 Hz, and the Allan deviation can reach 1.4×10^{-13}@1 s and 1.1×10^{-14}@100 s. We then measure the stability of the 20th comb tooth as shown in Fig. 3(e); the standard deviation is 24.81 Hz. The Allan deviation is at the same level as that of the pump laser, which is 1.4×10^{-13}@1 s and 1.1×10^{-14}@100 s. In contrast, the stabilities of the pump laser and the 20th comb tooth are all above 10^{-10} in the free-running case, as shown in Fig. 3(f). These results show that our microcomb has been fully locked to the hydrogen maser.

2.2 Precise and Rapid Distance Measurement with Hybrid Comb Lasers

In the distance meter, the microcomb serves as the signal source, which is split into the measurement arm and the reference arm. The fiber comb operates as the LO. Two PDs are used to detect the optical interferograms. We carried out absolute distance measurement in our lab; the results are shown in Fig. 4. The environmental conditions are 25.1°C, 98.7 kPa, and 53.1% humidity, and the group refractive index of air is 1.00026026 corrected by the Ciddor formula.[55] Figure 4(a) shows the interferograms of the hybrid-comb interferometry, and we find that the update rate is about 245.537 kHz, which is determined by the repetition frequencies of the microcomb and the fiber comb. In our experiments, the repetition frequency of the fiber comb $f_{\text{rep,FC}}$ is 249.711929 MHz, and that of the microcomb $f_{\text{rep,MC}}$ is 48.943783800 GHz after injection locking, which is about 196 times $f_{\text{rep,FC}}$. The Fourier transform of the interferograms is shown in Fig. 4(b), and a microwave comb can be obtained with 245.537 kHz frequency separation. The power of the center frequency at 12 MHz is relatively lower because the pump laser is degraded. We measure the distance for a relatively long term; the results are shown in Fig. 4(c). Figure 4(d) shows the comparison to the reference interferometer with a 0.05-m step size. At each position, the distances are fast-measured 10 times. The black solid points show the differences between the average of 10 individual measurements and the reference values, and the
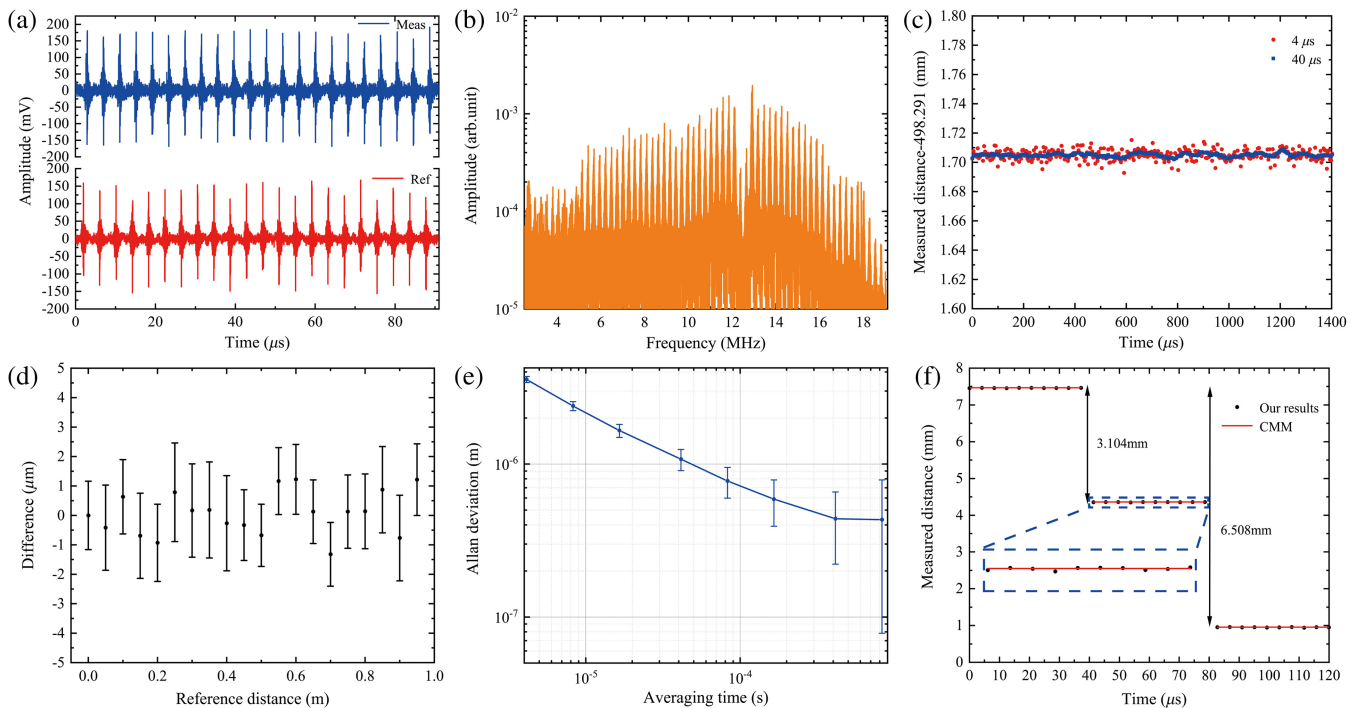

Fig. 4 Experimental results. (a) Interferograms of the hybrid-comb interferometry. (b) Fourier transform of the interferograms. (c) Ranging results at a standoff distance of 0.5 m. The red points indicate the results when the measuring time for the single measurement is 4 μs, and the blue line represents the results with 40 μs averaging time. (d) Results of the distance measurement. (e) Allan deviation measured at the distance of 0.5 m. (f) Measured surface profile of the disk. The black points show the measurement results and the red lines are the results measured by CMM.

error bar shows the standard deviation with an averaging time of 40 μs. The uncertainty can be within 2.5 μm in the 1-m range limited by the space of our lab. The Allan deviation can reach 3.572 μm at 4.136 μs (i.e., 245.537 kHz update rate), and further can be improved to 432 nm at 827.2 μs averaging time (i.e., 1.208 kHz update rate), showing that our system can support submicrometer precision and rapid distance measurement in Fig. 4(e). The uncertainty evaluation can be seen in Sec. 4.

To examine the ability of the rapid distance measurement, we measure a spin disk with grooves of different depths. The radius of the disk is about 15 cm, and the rotation speed is about 10,000 r/min. Therefore, the line speed of the disk edge can reach about 150 m/s. The results are shown in Fig. 4(f), and the grooves with 3.104 and 6.508 mm depths can be clearly captured. We use the measurement results of the coordinate measuring machine (CMM, Leica PMM-Ultra) as the reference values, and the measurement uncertainty can be within 2.5 μm.

3 Discussion and Conclusion

Submicrometer measurement mainly serves precision manufacturing and micromachining technology to characterize the geometric and mechanical properties of microstructures. The effect of geometric manufacturing accuracy on the final performance is nonlinear. Any precision mismatches between parts or components in the process of manufacturing sequence will transfer to the whole machine. It is necessary to have the measurement capability of large-range, high-precision, highly dynamic, real-time monitoring of the whole process. On the other hand, the changes of material properties, geometric structure, environmental conditions, and other factors due to the stress should be monitored in real time to avoid the overall performance of putting the equipment out of control. Furthermore, the establishment of a complete submicrometer measurement traceability system is a guarantee for high-tech industries, advanced manufacturing, and scientific development. Microcombs, the chip-scale comb lasers, have been finding increasing applications, from spectroscopy to precision measurement and metrology. Together with the rapid progress of microcombs, fiber combs are becoming mature and user-friendly nowadays. We, for the first time we believe, have developed a hybrid-comb distance meter that allows for high precision and high-speed ranging. Our hybrid strategy can utilize the merit of the microcombs, leading to ultrarapid distance measurement (hundreds of kilohertz or megahertz update rate). It can also operate in a fully stabilized manner, benefiting from the locking scheme of the fiber comb. Our results indicate the high coherence between the two types of combs (even a large repetition frequency difference exists), and the precision can reach the submicrometer level with coherent averaging. Nowadays, on-chip high gain waveguides or semiconductor optical amplifiers have been well developed, which can replace the gain fiber to realize compact mode-locked laser-based OFCs.[56,57] The gain waveguides could be integrated with a high-quality microcavity for integrated dual-hybrid comb formation. Viewed more broadly, the hybrid technique is universally applicable for different kinds of combs, and our work can provide a new insight into the technique of dual-comb interferometry, potentially giving rise to the promotion of its overall performance.

In conclusion, we develop a fully stabilized microcomb source with the help of one fiber comb. The f_{rep} of 48.943783800 GHz is actively stabilized by injection locking

with a 1.5 mHz standard deviation, and the relative stability can reach 3.1×10^{-14}@1 s and 2.4×10^{-15}@100 s. The pump laser (actually one tooth of the microcomb) is locked to one tooth of the fiber comb, and consequently, all the comb teeth have been referenced to the hydrogen maser. We measure the 20th tooth with respect to the pump laser to evaluate the locking performance. The results indicate the 24.81 Hz standard deviation, and the Allan deviation can achieve 1.4×10^{-13}@1 s and 1.1×10^{-14}@100 s. Since we include a fiber comb in our whole system, a hybrid-comb source with high coherence has been inherently obtained. Subsequently, we carry out optical ranging using the dual-hybrid comb interferometry. As a result of the large effective difference between the repetition frequencies of the hybrid combs, the measurement speed can be enhanced by 196 folds (i.e., $f_{\mathrm{rep,MC}}/f_{\mathrm{rep,FC}}$), in contrast to the dual-fiber-comb system with about 250 MHz repetition rate. The experimental results show the submicrometer precision in the distance measurement, and a fast spinning disk with about 150 m/s can be clearly measured, representing the rapid measurement speed.

4 Appendix: Materials and Methods

4.1 Development of the Fully Stabilized Single SMC

The integrated add-drop high-Q MRR is fabricated on a CMOS-compatible, high-index doped silica glass platform and packaged in a butterfly package with a thermo-electric cooler. The cross sections of the ring and bus waveguides are both 2 μm $\times$ 3 μm. The MRR exhibits anomalous dispersion in the communication band. In our experiments, the auxiliary optical field and pump laser locate in the same TM mode and are counter-coupled into the MRR to realize thermal balance for the SMC generation. By sequentially decreasing and increasing the operation temperature, the soliton switching and annihilation can be clearly recognized from the optical spectra. The Q factors of TM00 mode are 1.69×10^6. The MRR is pigtailed with a standard fiber array with coupling loss of about 2.5 dB per facet and insert loss from other passive optical devices of about 2.0 dB. The operation temperature of the MRR can be precisely tuned through an external TEC controller.

In our experiments, the microcomb is pumped by a continuous-wave (CW) laser (NKT Koheras ADJUSTIK E15, 1560.49 nm wavelength, 100 Hz linewidth, 40 mW output power). The output of the CW laser is shifted by 100 MHz by the first AOM and works as the pump laser. In the phase-locking loop, the pump laser is combined with the fiber comb (Menlo Systems FC1500, 1560 nm center wavelength, 50 nm bandwidth, about 250 MHz repetition frequency) at a polarization beam splitter, and then diffracted at a grating. After a pinhole to improve the signal-to-noise ratio, a PD is used to detect the beat notes between the pump laser and the fiber comb. Consequently, the amplified beat is fed into a servo system (Moku Lab), to produce an error signal. Finally, the AOM and piezoelectric ceramic transducer inside the CW laser are employed as the actuating element to lock the pump laser frequency.

The injection-locking technique provides an easy way to stabilize the repetition frequency of the microcomb. The second-order sidebands of the EOM are utilized for repetition frequency injection locking. Therefore, the driving frequency of the EOM is one half of $f_{\mathrm{rep,MC}}$, i.e., 24.471891900 GHz in our experiments. A high-speed PD (Finisar XPDV2120RA, 50 GHz) is

used to detect the repetition frequency f_{rep}, which is mixed with the output of the signal generator (R&S SMF100B), and the intermediate frequency signal of the mixer is filtered out using a low-pass filter and measured by the phase noise analyzer (R&S FSWP26). The repetition frequency stability is evaluated by a frequency counter (Keysight 53230A).

Subsequently, we use an additional fiber comb to evaluate the frequency stability of the microcomb lines. Taking the 20th comb tooth as an example, an optical tunable filter (SATEC OTF-950) is used to pick up the individual mode, which is then amplified and beats with the additional fiber comb. Finally, the beat note is used to measure the long-term stability and the SSB phase noise.

4.2 Distance Measurement Using Hybrid Comb Lasers

We have developed a fully stabilized microcomb source, and one self-referenced fiber comb is involved so as to lock the pump laser. Here, we actually have gotten one set of dual-comb sources with high coherence. In general, dual-comb interferometry, which has been widely used in metrology and spectroscopy, relies on two frequency combs with slightly different repetition frequencies. For example, the repetition frequency difference is several kilohertz for the fiber combs with f_{rep} of hundreds megahertz.[18] This value can be increased to several megahertz when the f_{rep} reaches tens of gigahertz in the cases of electro-optic combs[14,15] or microcombs.[38] In our work, one set of hybrid dual-comb sources can be naturally aroused, which comprises a microcomb ($f_{\text{rep,MC}}$, 48.943783800 GHz) and a fiber comb ($f_{\text{rep,FC}}$, 249.711929 MHz). The distances can be precisely determined using this hybrid dual-comb source, despite the large repetition frequency difference. We note that dual-comb interferometry with quasi-integer-ratio repetition rates has been previously described.[58,59] Nonetheless, we report here the coherent dual-hybrid-comb interferometry for distance measurement for the first time. The comparison among the different schemes of dual-comb interferometry is shown in Fig. 5. Table 1 shows the comparison with other dual-comb ranging methods.

In the distance measurement, the amplified microcomb is split into two parts. One part is used as a measurement beam after passing through the circulator, and the other part is the reference arm. The fiber comb actually serves as the LO. Two PDs are exploited to detect the interferograms, which are measured by an oscilloscope (LeCroy HDO6104A).

Assuming the field E_{MC} of the microcomb can be expressed as

$$E_{\text{MC}} = \sum_{p} A_{p,\text{MC}} \exp[2\pi i(p \times f_{\text{rep,MC}} + f_{\text{pump,MC}})t + i\varphi_{0,\text{MC}}],$$
(1)

where p is the relative mode number with respect to the pump resonance mode, $A_{p,\text{MC}}$ is the field amplitude of the pth comb tooth, $f_{\text{rep,MC}}$ is the repetition frequency of the microcomb, $f_{\text{pump,MC}}$ is the pump laser frequency of the microcomb, and $\varphi_{0,\text{MC}}$ is the initial phase.

Similarly, the field E_{FC} of the fiber comb can be written as

$$E_{\text{FC}} = \sum_{q} A_{q,\text{FC}} \exp[2\pi i(q \times f_{\text{rep,FC}} + f_{\text{center,FC}})t + i\varphi_{0,\text{FC}}],$$
(2)

where $A_{q,\text{FC}}$ is the field amplitude of the qth comb tooth, $f_{\text{rep,FC}}$ is the repetition frequency of the fiber comb, $f_{\text{center,FC}}$ is the center frequency of the fiber comb, $\varphi_{0,\text{FC}}$ is the initial phase, and q is the relative mode number with respect to the center frequency of the fiber comb. For the convenience of description, we assume that $f_{\text{pump,MC}}$ is close to $f_{\text{center,FC}}$, with the beat of f_b. Consequently, the heterodyne frequencies between the microcomb and the fiber comb can be expressed as

$$\begin{aligned} E_{\text{beat}} &\propto \sum_{p} \sum_{q} A_{p,\text{MC}} A_{q,\text{FC}} \exp[2\pi i(p \times f_{\text{rep,MC}} - q \times f_{\text{rep,FC}} \\ &\quad + f_{\text{pump,FC}} - f_{\text{center,FC}})t + i\varphi_{0,\text{MC}} - i\varphi_{0,\text{FC}}] \\ &\propto \sum_{p} \sum_{q} \exp[2\pi i(p \times f_{\text{rep,MC}} - q \times f_{\text{rep,FC}} + f_b)t \\ &\quad + i\varphi_{0,\text{MC}} - i\varphi_{0,\text{FC}}]. \end{aligned}$$
(3)

A number of beat notes can be obtained based on Eq. (3). In our experiments, $f_{\text{rep,MC}}$ is 48.943783800 GHz, and $f_{\text{rep,FC}}$ equals 249.711929 MHz, with the ratio of 196 (i.e., round $(f_{\text{rep,MC}}/f_{\text{rep,FC}})$, and round means the nearest integer). First, we consider the mode $f_{\text{pump,MC}} + f_{\text{rep,MC}}$ (the first mode), and correspondingly, the nearest mode in the fiber comb goes to $f_{\text{center,FC}} + 196 \times f_{\text{rep,FC}}$. The beat frequency can be calculated by $f_b + f_{\text{rep,MC}} - 196 \times f_{\text{rep,FC}}$. Let us go further and consider the second mode of the microcomb (i.e., $f_{\text{pump,MC}} + 2 \times f_{\text{rep,MC}}$). The nearest mode in the fiber comb is then $f_{\text{center,FC}} + 2 \times 196 \times f_{\text{rep,FC}}$, and the beat frequency is then $f_b + 2 \times (f_{\text{rep,MC}} - 196 \times f_{\text{rep,FC}})$. Consequently, we can reach a group of beat notes, which can be expressed as $f_b \pm p \times (f_{\text{rep,MC}} - 196 \times f_{\text{rep,FC}})$ ($p \sim \pm 100$). We find that all the microcomb modes can be downconverted to the radio frequency (RF) region by multiheterodyne interferometry. f_b can be easily tuned by the phase-locking loop, which is 12 MHz in our experiments. The value of $f_{\text{rep,MC}} - 196 \times f_{\text{rep,FC}}$ is 245.537 kHz, which is actually the frequency separation of this RF comb. To avoid spectral leakage, f_b is recommended to be larger than $p \times (f_{\text{rep,MC}} - 196 \times f_{\text{rep,FC}})$.

In fact, the mode $f_{\text{pump,MC}}$ can beat with all the modes of the fiber comb within the PD band. Considering the situation that $f_{\text{pump,MC}}$ beats with the mode of $f_{\text{center,FC}} + f_{\text{rep,FC}}$, the beat frequency f_b is then updated to $f_b + f_{\text{rep,FC}}$. Similarly, a new group of beat notes can make an appearance, which can be written as $f_b + f_{\text{rep,FC}} \pm p \times (f_{\text{rep,MC}} - 196 \times f_{\text{rep,FC}})$. In addition, if $f_{\text{pump,MC}}$ beats with the mode of $f_{\text{center,FC}} - f_{\text{rep,FC}}$, the beat frequency will be $f_{\text{rep,FC}} - f_b$, and in consequence, the corresponding group of beat notes can be expressed as $f_{\text{rep,FC}} - f_b \pm p \times (f_{\text{rep,MC}} - 196 \times f_{\text{rep,FC}})$. Finally, a series of groups of beat frequency, at different center frequencies but with the same frequency spacing, can be produced as shown in Fig. 5(e). The center frequency can be defined as $f_b + m \times f_{\text{rep,FC}}$ and $m \times f_{\text{rep,FC}} - f_b$ and is smaller than $f_{\text{rep,MC}}/2$. m is an integer. We note that, despite the groups of the beats located at the different frequencies along the frequency axis, each group can actually be individually picked up and utilized to determine the distances. In our experiments, we use a low-pass filter (DC-50MHz) to acquire the group at the center frequency of f_b.

In the time domain, the fiber comb scans the microcomb, like the optical sampling, to generate the interferograms. The
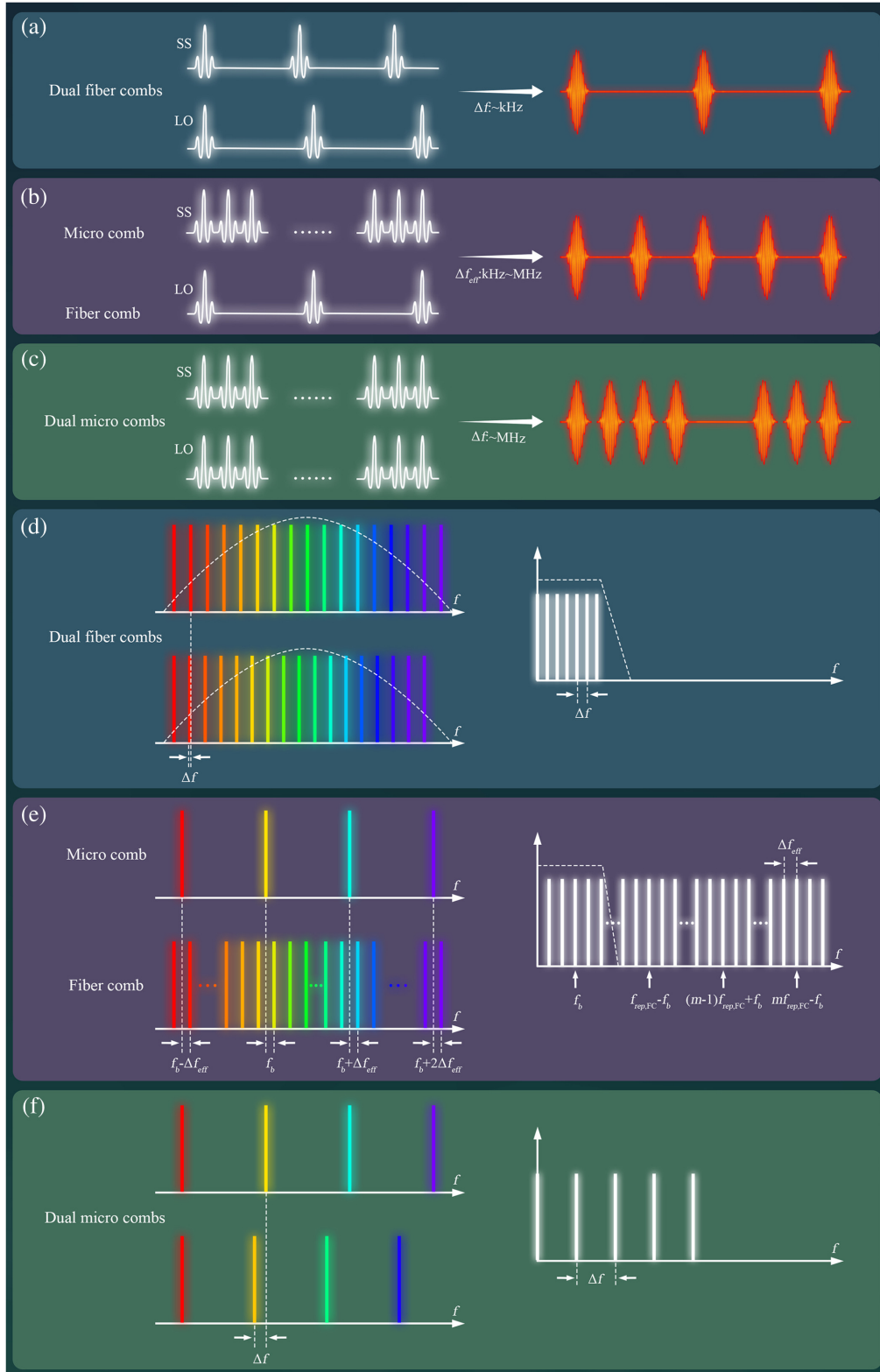
Fig. 5 The interferometry characteristics of different types of dual-comb sources. (a) Time-domain description of dual-fiber-comb interferometry. The difference between the repetition frequencies of the signal source (SS) and LO is often at the kilohertz level, implying that the update of the distance measurement is at the kilohertz level. The advantage of this system is that it is relatively easy to develop two fully stabilized fiber combs. (b) Time-domain description of hybrid-comb interferometry. The f_{rep} of the microcomb is usually high at the gigahertz level, or even at the terahertz level, and in contrast, the fiber comb often holds tens or hundreds of megahertz repetition frequency.

Fig. 5 (*Continued*) In spite of this highly different repetition frequency, hybrid-comb interferometry can occur. With the aid of the self-referenced fiber comb, the microcomb can be fully stabilized. In addition, the update rate can reach hundreds of kilohertz, or even megahertz, which is capable of rapid measurement. (c) Time-domain description of dual-microcomb interferometry. Since the high f_{rep}, the detuning between the repetition frequencies of SS and LO can easily reach tens of megahertz. Consequently, the update rate can also achieve tens of megahertz, showing the capability of ultrafast measurement. However, it is rather challenging to fully stabilize two microcombs without the help of the self-referenced fiber comb. (d) Frequency-domain description of dual-fiber-comb interferometry. Because of the (relatively) small repetition frequency and the broad optical band, the optical band pass filter is generally required to circumvent the spectrum aliasing. The beat notes should be smaller than $f_{\mathrm{rep}}/2$, with a frequency separation of Δf. Δf is the difference between the repetition frequencies. (e) Frequency-domain description of hybrid-comb interferometry. Interestingly, the beat components are composed of a series of groups with different center frequencies. An electrical filter can be used to select the different groups of the beat notes, whose phases can be used to calculate the distances. (f) Frequency-domain description of dual-microcomb interferometry. Similar to dual-fiber-comb interferometry, the beat notes are located with the separation of Δf. The optical bandpass filter is not strictly required since the repetition frequency of microcomb is large.

Table 1 Comparison with other dual-comb ranging methods.

Type	Stabilization	Precision	Update rate	Reference
Dual-fiber combs	f_{rep} locked	38.8 μm@200 μs	5 kHz	Ref. 16
	Unlocked	10 μm@50 ms	20 Hz	Ref. 17
	Unlocked	290 nm@1.5 ms	666 Hz	Ref. 20
	Unlocked	900 nm@5 μs	200 kHz	Ref. 24
	f_{rep} locked	1.48 μm@500 μs	2 kHz	Ref. 58
Dual electro-optic (EO) combs	f_{rep} locked	2 μm@9.1 μs	110 kHz	Ref. 14
	f_{rep} locked	5 μm@14 μs	71 kHz	Ref. 15
Triple EO combs	f_{rep} locked	10 μm@2 μs	500 kHz	Ref. 57
Dual micro combs	Unlocked	284 nm@10.4 ns	96 MHz	Ref. 38
	Unlocked	8 μm@176 μs	5.685 kHz	Ref. 39
Hybrid combs (one micro comb, one fiber comb)	Fully locked	3.572 μm@4.136 μs	245.537 kHz	This work

difference is that $f_{\mathrm{rep,MC}}$ is not slightly detuned with $f_{\mathrm{rep,FC}}$, but is much larger than $f_{\mathrm{rep,FC}}$ (196 times). As a result, 196 interferograms can be generated, when the fiber comb (LO) scans $1/f_{\mathrm{rep,FC}}$ in the time line. In contrast to the dual-fiber-comb interferometry, one interferogram appears with each scan of $1/f_{\mathrm{rep,FC}}$. Therefore, the measuring speed (the update rate) can be enhanced by 196 folds, corresponding to the frequency separation of $f_{\mathrm{rep,MC}} - 196 \times f_{\mathrm{rep,FC}}$ in the frequency domain.

In our ranging system, the distance can be calculated as

$$
\begin{aligned}
L &= \frac{1}{2} \cdot \frac{c}{n_g} \cdot \left(\frac{N}{f_{\mathrm{rep,MC}}} + \tau \cdot \frac{f_{\mathrm{rep,MC}} - 196 \times f_{\mathrm{rep,FC}}}{f_{\mathrm{rep,MC}}} \right) \\
&= \frac{1}{2} \cdot \frac{c}{n_g \cdot f_{\mathrm{rep,MC}}} \cdot (N + \tau \times \Delta f_{\mathrm{eff}}),
\end{aligned}
\tag{4}
$$

where we define the parameter $f_{\mathrm{rep,MC}} - 196 \times f_{\mathrm{rep,FC}}$ as the effective repetition frequency difference, which is referred to as Δf_{eff}. N is the integer part of the pulse-to-pulse length, c is the light speed in vacuum, and n_g is the group refractive index of air. τ is the real-time delay, which can be measured by Hilbert transform or Fourier transform.

4.3 Uncertainty Budget

In Eq. (4), the integer N can be precisely determined with uncertainty below 0.5 by changing the repetition frequency of the microcomb,[60] and thus will not contribute to the measurement uncertainty. Consequently, the measurement uncertainty of the distance measurement is related to the parameters of the group refractive index n_g, the repetition frequency of the microcomb $f_{\mathrm{rep,MC}}$, the real-time delay τ, and the effective repetition frequency difference Δf_{eff}, as calculated in the following equation:

$$
\begin{aligned}
u_L^2 &= \left(\frac{\partial L}{\partial n_g} u_{n_g} \right)^2 + \left(\frac{\partial L}{\partial f_{\mathrm{rep,MC}}} u_{f_{\mathrm{rep,MC}}} \right)^2 + \left(\frac{\partial L}{\partial \tau} u_\tau \right)^2 \\
&\quad + \left(\frac{\partial L}{\partial \Delta f_{\mathrm{eff}}} u_{\Delta f_{\mathrm{eff}}} \right)^2 \\
&= \left(\frac{L}{n_g} u_{n_g} \right)^2 + \left(\frac{L}{f_{\mathrm{rep,MC}}} u_{f_{\mathrm{rep,MC}}} \right)^2 + \left(\frac{1}{2} \cdot \frac{c}{n_g} \cdot \frac{\Delta f_{\mathrm{eff}}}{f_{\mathrm{rep,MC}}} u_\tau \right)^2 \\
&\quad + \left(\frac{1}{2} \cdot \frac{c}{n_g} \cdot \frac{\tau}{f_{\mathrm{rep,MC}}} u_{\Delta f_{\mathrm{eff}}} \right)^2.
\end{aligned}
\tag{5}
$$

The first term on the right side is due to the group refractive index of air. In general, the measurement of the air refractive index is based on the empirical equation (Ciddor formula in this work) using environmental sensors. The uncertainty of the Ciddor formula itself is about 2×10^{-8}. The measurement uncertainties of the temperature, the pressure, and the relative humidity are determined by the uncertainties of the sensors, the environmental stability, and the homogeneity, which turns out to be 27 mK, 13 Pa, and 1.7%, respectively. Correspondingly, the uncertainties due to the measurement of the environmental parameters are 2.5×10^{-8}, 3.3×10^{-8}, and 2×10^{-8}, respectively. Therefore, the uncertainty of n_g can be combined to be 5×10^{-8}. The second term is related to the uncertainty of the repetition frequency, which is well-locked to the hydrogen maser. Since the stability of the hydrogen maser is better than 10^{-13} at 1 s averaging time, this part can be estimated as $10^{-13} \cdot L$, which can be neglected in fact. The third term is due to the measurement of the real-time delay, which can be evaluated by the standard deviation. In our experiments, the standard deviation can reach 1.7 μm with 40 μs averaging time. We note that the part can also include the effect due to the fiber fluctuation and the stage vibration, despite the fact that we place the devices into a well-controlled enclosure. The last term is due to the uncertainty of the parameter Δf_{eff}. Here, we can give an upper limit of the fourth term, where τ equals $1/\Delta f_{\text{eff}}$ (i.e., the maximum value). Δf_{eff} is equal to $f_{\text{rep,MC}} - 196 \times f_{\text{rep,FC}}$, and both $f_{\text{rep,MC}}$ and $f_{\text{rep,FC}}$ are locked to the hydrogen maser. Therefore, the uncertainty of Δf_{eff} can be also better than 10^{-13}. $f_{\text{rep,MC}}$ is about 50 GHz. In this case, the fourth term is at 10^{-16} m level, which can be neglected. Since the micro-comb laser and the reference distance meter do not share the same target mirror, an Abbe error could exist. The Abbe error is always below 2 μm during the whole stroke, corresponding to a 20 μrad yaw error of the rail. Finally, the combined uncertainty can be calculated as $[(2.6\ \mu\text{m})^2 + (5 \times 10^{-8} \cdot L)^2]^{0.5}$.

Disclosures

The authors declare that they have no conflicts of interest.

Code and Data Availability

The data that support the plots within this paper are available from the corresponding author upon reasonable request.

References

1. G. Berkovic and E. Shafir, "Optical methods for distance and displacement measurements," *Adv. Opt. Photonics* **4**, 441–471 (2012).
2. S. A. Diddams, K. Vahala, and T. Udem, "Optical frequency combs: coherently uniting the electromagnetic spectrum," *Science* **369**, 3676 (2020).
3. S. A. Diddams, "The evolving optical frequency comb [Invited]," *J. Opt. Soc. Am. B* **27**, B51–B62 (2010).
4. J. Ye, "Absolute measurement of a long, arbitrary distance to less than an optical fringe," *Opt. Lett.* **29**, 1153–1155 (2004).
5. H. Z. Wu et al., "Long distance measurement using optical sampling by cavity tuning," *Opt. Lett.* **41**, 2366–2369 (2016).
6. D. Wei et al., "Time-of-flight method using multiple pulse train interference as a time recorder," *Opt. Express* **19**, 4881–4889 (2011).
7. S. Han et al., "Absolute distance measurement by adjustable synthetic wavelength dual-comb interferometry," in *CLEO: OSA Tech. Digest (online)*, Optica Publishing Group, p. CTu2I.8 (2013).
8. H. Z. Wu et al., "Absolute distance measurement with correction of air refractive index by using two-color dispersive interferometry," *Opt. Express* **24**, 24361–24376 (2016).
9. M. Cui et al., "Long distance measurement with femtosecond pulses using a dispersive interferometer," *Opt. Express* **19**, 6549–6562 (2011).
10. X. Liang et al., "Optical frequency comb frequency-division multiplexing dispersive interference multichannel distance measurement," *Nanomanuf. Metrol.* **6**, 6 (2023).
11. R. D. Nicolae et al., "Absolute distance measurement system using a femtosecond laser as a modulator," *Meas. Sci. Technol.* **21**, 115302 (2010).
12. K. Minoshima and H. Matsumoto, "High-accuracy measurement of 240-m distance in an optical tunnel by use of a compact femtosecond laser," *Appl. Opt.* **39**, 5512–5517 (2000).
13. R. T. Yang et al., "Absolute distance measurement by dual-comb interferometry with multi-channel digital lock-in phase detection," *Meas. Sci. Technol.* **26**, 084001 (2015).
14. C. Weimann et al., "Fast high-precision distance metrology using a pair of modulator-generated dual-color frequency combs," *Opt. Express* **26**, 34305–34335 (2018).
15. C. Weimann et al., "Silicon photonic integrated circuit for fast and precise dual-comb distance metrology," *Opt. Express* **25**, 30091–30104 (2017).
16. J. Lee et al., "Absolute distance measurement by dual-comb interferometry with adjustable synthetic wavelength," *Meas. Sci. Technol.* **24**, 045201 (2013).
17. D. T. Hu et al., "Dual-comb absolute distance measurement of non-cooperative targets with a single free-running mode-locked fiber laser," *Opt. Commun.* **482**, 126566 (2021).
18. Z. B. Zhu and G. H. Wu, "Dual-comb ranging," *Engineering* **4**, 772–778 (2018).
19. S. Y. Zhou et al., "Dual-comb spectroscopy resolved three-degree-of-freedom sensing," *Photonics Res.* **9**, 243 (2021).
20. S. L. Camenzind et al., "Dynamic and precise long-distance ranging using a free-running dual-comb laser," *Opt. Express* **30**, 37245–37260 (2022).
21. H. Wright et al., "Two-photon dual-comb LiDAR," in *Conf. Lasers and Electro-Opt., Tech. Digest Ser.*, Optica Publishing Group, p. SS1A.1 (2022).
22. I. Coddington, et al., "Rapid and precise absolute distance measurements at long range," *Nat. Photonics* **3**, 351–356 (2009).
23. E. D. Caldwell et al., "The time-programmable frequency comb and its use in quantum-limited ranging," *Nature* **610**, 667–673 (2022).
24. Z. Wu et al., "High-precision surface profilometry on a microngroove based on dual-comb electronically controlled optical sampling," *Appl. Opt.* **62**, 8793–8797 (2023).
25. J. Lee et al., "Time-of-flight measurement with femtosecond light pulses," *Nat. Photonics* **4**, 716–720 (2010).
26. Y. J. Na et al., "Ultrafast, sub-nanometre-precision and multifunctional time-of-flight detection," *Nat. Photonics* **14**, 355–360 (2020).
27. T. Fortier and E. Baumann, "20 years of developments in optical frequency comb technology and applications," *Commun. Phys.* **2**, 153 (2019).
28. R. J. Zhuang et al., "Electro-optic frequency combs: theory, characteristics, and applications," *Laser Photonics Rev* **17**, 2200353 (2023).

29. V. Torres-Company and A. M. Weiner, "Optical frequency comb technology for ultra-broadband radio-frequency photonics," *Laser Photonics Rev.* **8**, 368–393 (2014).

30. P. Alexandre et al., "Dual-comb interferometry for coherence analysis of tightly locked mid-infrared quantum cascade laser frequency combs," *Adv. Photon. Res.* 2400006 (2024).

31. W. Q. Wang, L. R. Wang, and W. F. Zhang, "Advances in soliton microcomb generation," *Adv. Photonics* **2**, 034001 (2020).

32. S. W. Huang et al., "A broadband chip-scale optical frequency synthesizer at 2.7×10^{-16} relative uncertainty," *Sci. Adv.* **2**, 1501489 (2016).

33. T. J. Kippenberg et al., "Dissipative Kerr solitons in optical microresonators," *Science* **361**, eaan8083 (2018).

34. A. Pasquazi et al., "Micro-combs: a novel generation of optical sources," *Phys. Rep.* **729**, 1–81 (2018).

35. J. H. Zheng et al., "Optical ranging system based on multiple pulse train interference using soliton microcomb," *Appl. Phys. Lett.* **118**, 261106 (2021).

36. J. D. Wang et al., "Long-distance ranging with high precision using a soliton microcomb," *Photonics Res.* **8**, 1964 (2020).

37. Y. S. Jang et al., "Nanometric precision distance metrology via hybrid spectrally resolved and homodyne interferometry in a single soliton frequency microcomb," *Phys. Rev. Lett.* **126**, 023903 (2021).

38. P. Trocha et al., "Ultrafast optical ranging using microresonator soliton frequency combs," *Science* **359**, 887–891 (2018).

39. M. G. Suh and K. J. Vahala, "Soliton microcomb range measurement," *Science* **359**, 884–887 (2018).

40. J. Riemensberger et al., "Massively parallel coherent laser ranging using a soliton microcomb," *Nature* **581**, 164–170 (2020).

41. A. Lukashchuk et al., "Dual chirped microcomb based parallel ranging at megapixel-line rates," *Nat. Commun.* **13**, 3280 (2022).

42. L. H. Jia et al., "Nonlinear calibration of frequency modulated continuous wave LIDAR based on a microresonator soliton comb," *Opt. Lett.* **46**, 1025–1028 (2021).

43. R. X. Chen et al., "Breaking the temporal and frequency congestion of LiDAR by parallel chaos," *Nat. Photonics* **17**, 306–314 (2023).

44. A. Lukashchuk et al., "Chaotic microcomb-based parallel ranging," *Nat. Photonics* **17**, 814–821 (2023).

45. P. Del'Haye et al., "Phase-coherent microwave-to-optical link with a self-referenced microcomb," *Nat. Photonics* **10**, 516–520 (2016).

46. V. Brasch et al., "Self-referenced photonic chip soliton Kerr frequency comb," *Light Sci. Appl.* **6**, e16202 (2017).

47. Z. L. Newman et al., "Architecture for the photonic integration of an optical atomic clock," *Optica* **6**, 680–685 (2019).

48. P. Del'Haye et al., "Full stabilization of a microresonator-based optical frequency comb," *Phys. Rev. Lett.* **101**, 053903 (2008).

49. J. D. Jost et al., "All-optical stabilization of a soliton frequency comb in a crystalline microresonator," *Opt. Lett.* **40**, 4723–4726 (2015).

50. W. Weng et al., "Spectral purification of microwave signals with disciplined dissipative Kerr solitons," *Phys. Rev. Lett.* **122**, 013902 (2019).

51. L. Stern et al., "Direct Kerr frequency comb atomic spectroscopy and stabilization," *Sci. Adv.* **6**, eaax6230 (2020).

52. X. W. Liu et al., "Aluminum nitride nanophotonics for beyond-octave soliton microcomb generation and self-referencing," *Nat. Commun.* **12**, 5428 (2021).

53. P. Del'Haye et al., "Octave spanning tunable frequency comb from a microresonator," *Phys. Rev. Lett.* **107**, 063901 (2011).

54. P. A. Williams, W. C. Swann, and N. R. Newbury, "High-stability transfer of an optical frequency over long fiber-optic links," *J. Opt. Soc. Am. B* **25**, 1284–1293 (2008).

55. P. E. Ciddor, "Refractive index of air: new equations for the visible and near infrared," *Appl. Opt.* **35**, 1566–1573 (1996).

56. J. Rönn et al., "Ultra-high on-chip optical gain in erbium-based hybrid slot waveguides," *Nat. Commun.* **10**, 432 (2019).

57. S. T. Liu et al., "High-performance O-band quantum-dot semiconductor optical amplifiers directly grown on a CMOS compatible silicon substrate," *ACS Photonics* **6**, 2523–2529 (2019).

58. N. B. Hébert et al., "Coherent dual-comb interferometry with quasi-integer-ratio repetition rates," *Opt. Express* **22**, 29152–29160 (2014).

59. R. Li et al., "Ultra-rapid dual-comb ranging with an extended non-ambiguity range," *Opt. Lett.* **47**, 5309–5312 (2022).

60. H. Y. Zhang et al., "Absolute distance measurement by dual-comb nonlinear asynchronous optical sampling," *Opt. Express* **22**, 6597–6604 (2014).

Biographies of the authors are not available.